

PERFORMANCE EVALUATION OF AUTOMATED AND MANUAL SEISMIC PHASE PICKING FOR RAPID EARTHQUAKE PARAMETER DETERMINATION IN THE INDONESIAN BMKG NETWORK

Rayhan Irfan Hielmy^{1*}, Bayu Pranata², Wijayanto², Daryono²

¹Geophysics Department, State College of Meteorological, Climatological, and Geophysics, Indonesia

²Indonesian Agency for Meteorological, Climatological and Geophysics, Indonesia.

*E-mail: rayhanirfanhielmy1@gmail.com

Received: September 19, 2025

Reviewed: October 24, 2025

Accepted: November 19, 2025

ABSTRACT

Indonesia is located at the intersection of three major tectonic plates, which causes high seismic activity and vulnerability to earthquakes. Determining the initial parameters of an earthquake, such as the time of occurrence, epicenter location, depth, and magnitude, is very important for early warning systems. This study compares the performance of automatic selection and fast manual selection (<3 minutes, S-wave-based) with final validated results to evaluate the reliability of both methods. Data were obtained from the BMKG SeisComP system for the period May 18, 2024–May 17, 2025, covering 2,790 earthquake events across Indonesia, including analysis of areas with lower seismicity like Kalimantan. Analysis was conducted on six main parameters (depth, origin time, RMS, azimuth gap, magnitude, and earthquake center), which were evaluated using a numerical scoring system (0-100) based on their deviation from final validated data to allow for quality assessment and classification. Results show that automatic picking processed significantly more events (1,857 events, 66.6%) compared to manual picking (327 events, 11.7%) within the same timeframe. In terms of quality, manual picking achieved a higher proportion of 'good' category results (score 75–100) with 96.9%, compared to automatic picking's 88.5%. However, automatic picking remains preferable for rapid dissemination of earthquake information (<3 minutes) due to speed. The study also determines regional thresholds for the minimum number of seismic phases required for reliable automatic picking (Phase 8–16, depending on region, with a national average at Phase 15).

Keywords: Automatic Phase Picking, Manual Phase Picking, Earthquake Parameter, Indonesia, Early Warning Systems

1. Introduction

Indonesia is one of the most seismically active regions in the world, influenced by a highly complex tectonic system. As an archipelagic nation situated at the intersection of three active tectonic plates—the Eurasian Plate, the Indo-Australian Plate, and the Pacific Plate—Indonesia is constantly subjected to plate movements that collide or subduct into one another [1]. This condition makes Indonesia an active tectonic zone with a high level of seismicity. Generally, active tectonic locations in Indonesia can be identified along the boundaries of these plates. However, the impact of tectonic activity can be felt even in areas far from the epicenter, depending on the dissipation of earthquake energy and local geological conditions [2].

The impact of these tectonic dynamics is not limited to earthquakes, but also contributes to the formation of diverse geological structures, such as volcanic mountains, lowlands, and active faults that divide the Indonesian archipelago [3]. As a result, 28 regions in Indonesia are categorized as geologically hazardous areas, including tectonic earthquakes, volcanic

eruptions, and tsunamis. These regions include Nanggroe Aceh Darussalam (NAD), North Sumatra, West Sumatra, Bengkulu, Lampung, Banten, Central Java, the southern part of the Special Region of Yogyakarta, the southern part of East Java, Bali, West Nusa Tenggara (NTB), and East Nusa Tenggara (NTT) [4], [5].

In the context of disasters, initial estimates of earthquake parameters are crucial. These parameters include the time of occurrence, epicenter location, depth, and magnitude, which are important information for early warning systems, emergency response activation, and rapid decision-making by the government and affected communities. The accuracy and speed of obtaining these initial parameters greatly influence the effectiveness of disaster response.

In practice, SeisComP is used to determine earthquake parameters [6]. The automatic picking system in this software is often utilized to expedite the initial identification of seismic waves. The system works in real-time using algorithms such as STA/LTA, and generally focuses only on detecting P-waves. This process is usually carried out through the

Scautopick module in SeisComP [7], which applies STA/LTA detectors to automatically identify the arrival of P-waves [8].

The STA/LTA method itself is based on a simple principle, namely the ratio between the short-term average (STA) and long-term average (LTA) calculated continuously at each time for each data channel [9]. Although this method is rapid, it has well-known limitations. The STA/LTA algorithm is highly sensitive to background noise and transient signals, which can lead to a high rate of false positives or missed detections, particularly for smaller events. Furthermore, the standard algorithm is primarily designed for P-wave detection and struggles to reliably identify S-wave arrivals. This is a significant drawback, as S-waves are critical for accurately constraining earthquake depth and magnitude [10], [11]. As a result, the initial parameters generated automatically may differ significantly from the final results obtained through manual analysis by seismologists

Therefore, the picking process is performed manually, covering at least one S-wave, and completed as quickly as possible, usually within 3 minutes after the earthquake. The aim is to reduce errors that often occur in automatic picking that relies solely on P-waves, such as in determining the earthquake hypocenter based on the time difference between the arrival of P-waves and S-waves [10]. Additionally, S-waves are also useful for determining earthquake depth [11], while still allowing for rapid information dissemination.

However, time constraints often result in suboptimal data accuracy. On the other hand, manual picking, which is done more carefully and takes into account many wave phases, can produce more accurate earthquake data, although it takes longer. The differences in results between automatic picking, fast manual picking (less than 3 minutes), and the final results after in-depth analysis raise questions about the reliability of each method.

While this study focuses on the Indonesian BMKG network, its findings offer a valuable framework for other seismic monitoring agencies globally. The operational challenge of balancing the speed of automated alerts against the accuracy of manual review is universal. By quantifying the performance of these methods and establishing regional minimum-phase thresholds for reliable automatic solutions, this research provides a methodological template that can inform and improve rapid monitoring practices in other tectonically active regions. Therefore, this study aims to conduct two separate evaluations against the final results: (1) to assess the performance of automatic picking (< 3 min) and (2) to assess the performance of fast manual picking (< 3 min, with at least one S-wave). This study does not aim to directly

compare automatic vs. manual, but rather to evaluate each method's reliability independently.

2. Methods

We analyzed 2,790 earthquake events recorded by BMKG's SeisComP system between May 18, 2024, and May 17, 2025. Two approaches were compared: automatic picking and fast manual picking (<3 minutes, with at least one S-wave). Six parameters (origin time, depth, magnitude, RMS, azimuthal gap, and epicenter) were benchmarked against the validated final results. Events were classified into four quality categories (good, fair, poor, very poor) based on a scoring system. Regional analyses were conducted to determine the minimum number of seismic phases required for reliable automatic picking.

Sample data can be seen in Table 1. The OT column indicates the origin time or the time of the earthquake, while the Timesince column shows the time interval since the parameter was created. The Lat, Lon, and D columns describe the location of the earthquake, respectively, in the form of latitude, longitude, and depth. The Phs column records the number of seismic wave phases used. Azgap is the azimuth gap angle, which is the largest angle between two nearest seismic stations measured from the epicenter. The RMS (root mean square) column indicates the average error between the seismic wave travel time calculated by the model and the observed time [12]. The M and MLv columns reflect the magnitude values used. Mode indicates the data picking method, either manual or automatic.

Meanwhile, the Status column indicates the origin's validation level: undefined means it is the raw, unreviewed solution from the automatic system; confirmed means it has been manually processed (typically the <3 min solution) but is not yet final; and final means the final result of the manual process. This 'final' data serves as the 'ground truth' for this study and represents the official, published parameters derived from a comprehensive manual review by experienced BMKG seismologists. This final validation is conducted without the < 3-minute time constraint and often incorporates additional waveform analysis or stations.

In addition, phase data for each earthquake event were also obtained from the FDSNWS website. The data period analyzed covers May 18, 2024, to May 17, 2025. The study area covers the entire Indonesian archipelago, with coordinates ranging from 95° E to 141° E, and from 11° S to 6° N, in accordance with the coverage area specified in the BMKG repository. A total of 2,790 earthquake events were analyzed, with a relatively even distribution across the entire territory of Indonesia. However, the Kalimantan region exhibits lower seismicity compared to other regions, as shown in Figure 1.

Table 1 Data of event bmg2025jmix

OT	Timesince	Lat	Lon	De	Phs	Azgap	RMS	M	MLv	Mode	Status
2025-05-15 19:57:13	00:01:00	-1.22	121.27	10	11	88	0.61	2.97	2.98	automatic	undefined
2025-05-15 19:57:13	00:01:05	-1.22	121.28	10	12	78	0.75	3.02	3.03	automatic	undefined
2025-05-15 19:57:13	00:01:43	-1.21	121.25	10	24	97	1.01	3.03	3.04	manual	confirmed
2025-05-15 19:57:13	00:04:37	-1.22	121.28	10	12	78	0.75	3.02	3.03	automatic	undefined
2025-05-15 19:57:13	00:04:49	-1.23	121.29	10	13	68	0.95	3.67	3.04	automatic	undefined
2025-05-15 19:57:13	10:27:44	-1.21	121.25	5	34	100	0.85	3.03	3.04	manual	final

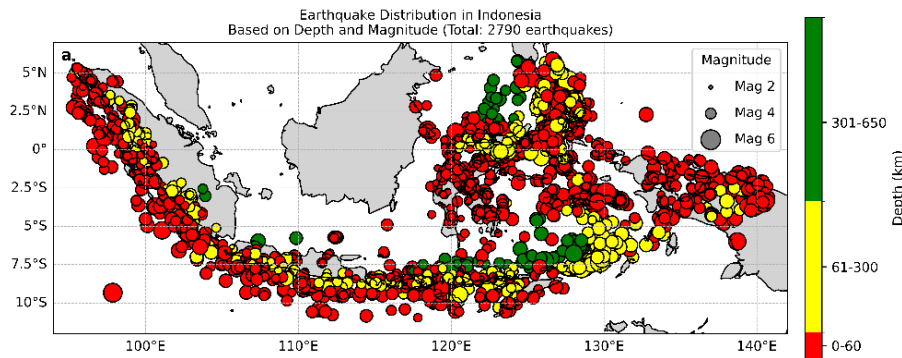


Figure 1 Earthquake distribution used in this study.

For magnitude, this study prioritized the system's preferred weighted average magnitude ('M') for earthquakes with a magnitude below 5, and moment magnitude (M_w) for those above 5. We selected 'M' as the primary metric because it represents the most stable, default magnitude provided by SeisComP in the rapid (< 3 min) operational workflow, which is the protocol being evaluated. In cases where the 'M' value was not available or robustly calculated, the local magnitude from vertical components (MLv) was used as a fallback.

Specialized software was used to support the research process. SeisComP was used to obtain earthquake data during the specified period. Meanwhile, Python was used for data processing, calculating the best parameters, and creating visualizations of earthquake distribution maps and analysis results. The calculation of the best parameters is done by comparing six parameters with the final data, namely

depth, origin time, RMS, azimuthal gap, magnitude, and epicenter. The difference value is calculated based on the difference between the analyzed results and the final data, using the formula:

$$Diff = Auto/Man Data - Final Data \quad (1)$$

Each parameter will be given a score based on the magnitude of the difference. The smaller the difference, the higher the score will be. The smallest difference is given a score of 100, while the largest difference is given a score of 0. If the difference value exceeds the maximum limit set for each parameter, the score will automatically be assigned a value of 0. The details of these provisions can be found in Table 2. Specifically for the depth parameter, if there is a change in the depth category (shallow, medium, or deep), the score will automatically be assigned a value of 0 without considering the magnitude of the difference.

Table 2 Range of values and scores

No	Parameter	Absolute Value	Score
1	RMS (seconds) (Min)	0	100
	RMS (seconds) (Max)	5	0
2	Azimuth Gap (degrees) (Min)	0	100
	Azimuth Gap (degrees) (Max)	360	0
3	Origin Time Difference (seconds) (Min)	0	100
	Origin Time Difference (seconds) (Max)	40	0
4	Magnitude Difference (M/MLv/Mw) (Min)	0	100
	Magnitude Difference (M/MLv/Mw) (Max)	1	0
5	Depth Difference (km) (Min)	0	100
	Depth Difference (km) (Max, if shallow)	60	0
	Depth Difference (km) (Max, if intermediate)	240	0
	Depth Difference (km) (Max, if deep)	350	0
6	Epicenter Difference (km) (Min)	0	100
	Epicenter Difference (km) (Max)	100	0

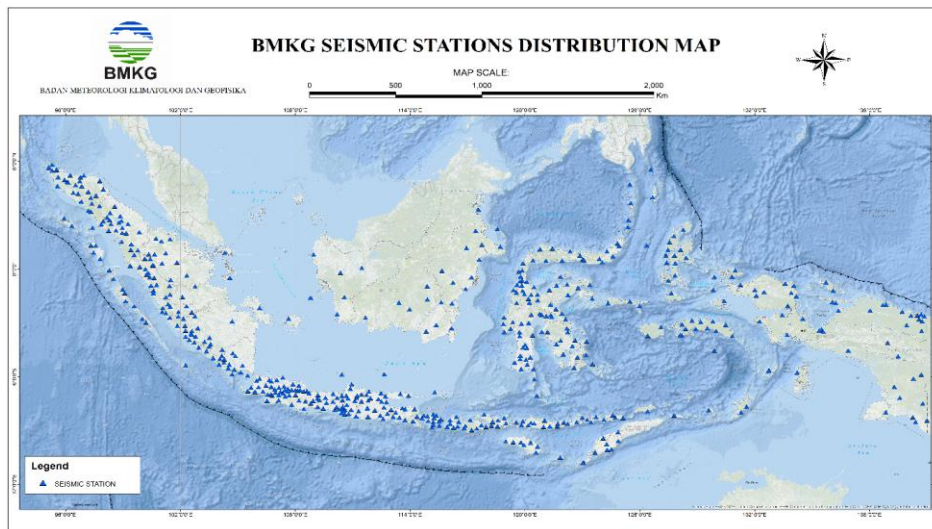


Figure 2. Map of the BMKG seismic station distribution used in this study

It must be emphasized that the maximum thresholds (the values for a score of 0) listed in Table 2 were established based on their operational relevance for rapid information dissemination. These values represent the maximum acceptable error tolerance, beyond which the initial information could be considered misleading for disaster response. For example, a magnitude error greater than 1.0 (e.g., reporting M4.5 when it is M5.5) fundamentally changes the perception of potential damage. Likewise, an epicenter error over 100 km could incorrectly shift the event from offshore (tsunami potential) to onshore, or into a different province. The depth parameter justification is the most critical: as stated previously, if a change in depth category (e.g., from 'shallow' to 'intermediate') occurs, the parameter automatically receives a score of 0, as this has direct and significant implications for shaking hazard and tsunami potential. Then, once all scores for each parameter have been obtained, the total average score will be calculated using the following equation:

$$Average\ Score = \frac{\sum Score}{6} \quad (2)$$

Once the average value has been obtained, the score will be classified into four quality categories, namely very poor, poor, fair, and good, as shown in Table 3. This classification is used to assess the quality of the results based on the degree of closeness of the parameters to the final data. The distribution of the BMKG seismic stations used in this study is shown in Figure 2. As seen, the density and geometry of the station network vary across the Indonesian archipelago. This station distribution is a critical factor influencing the number of recorded phases and the *azimuth gap* coverage, which will be discussed further in the 'Discussion' section.

Table 3 Classification of score

No	Category	Range of Score
1	Good	75 – 100
2	Fair	50 - 75
3	Poor	25 – 50
4	Very Poor	0 – 25

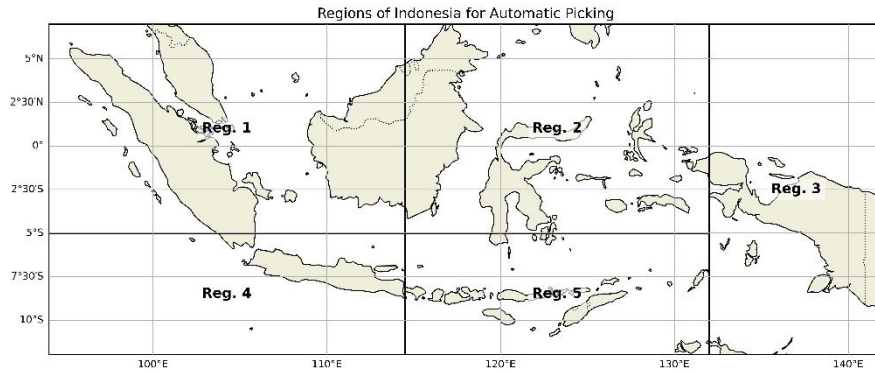


Figure 3. Regions of Indonesia for automatic picking

The data processing involves two distinct analyses: automatic picking and manual picking, both completed in less than 3 minutes (< 3 minutes). For the regional analysis, which focused only on automatic picking, the study area was divided into five regions based on seismicity distribution (see Figure 3). This division aims to determine the minimum number of phases required for automatic picking parameters to be categorized as “good.” This analysis exclusively used events with automatic picking information from the < 3 minute timeframe. In contrast, the analysis for manual picking (< 3 minutes) did not use regional divisions, as it focused on a smaller dataset of events that included at least one S wave.

3. Result and Discussion

Comparison of Automatic Picking. Based on Figures 4a–4b, the distribution of earthquakes in Indonesia with automatic picking times of less than 3 minutes (<3 minutes) recorded 1,857 events, or 66.6% of the total number of earthquakes. Of these,

shallow earthquakes (0–60 km) dominated with 1,328 events (71.5%), followed by intermediate earthquakes (60–300 km) with 456 events (24.6%), and deep earthquakes (300–650 km) with 73 events (3.9%).

Shallow and intermediate earthquakes were evenly distributed across almost the entire Indonesian territory, reflecting widespread seismic activity. Meanwhile, deep earthquakes were generally concentrated in the northern regions of Bali, West Nusa Tenggara (NTB), East Nusa Tenggara (NTT), and northern Sulawesi. The Kalimantan region did not show significant seismic activity. Meanwhile, based on Figures 4c–4d, the distribution of earthquakes based on picking quality scores is dominated by the good category (scores of 75–100) with 1,644 events (88.5%). The fair category (score 50–75) includes 161 earthquakes (8.7%), followed by poor (25–50) with 47 earthquakes (2.5%), and very poor (0–25) with only 5 earthquakes (0.3%).

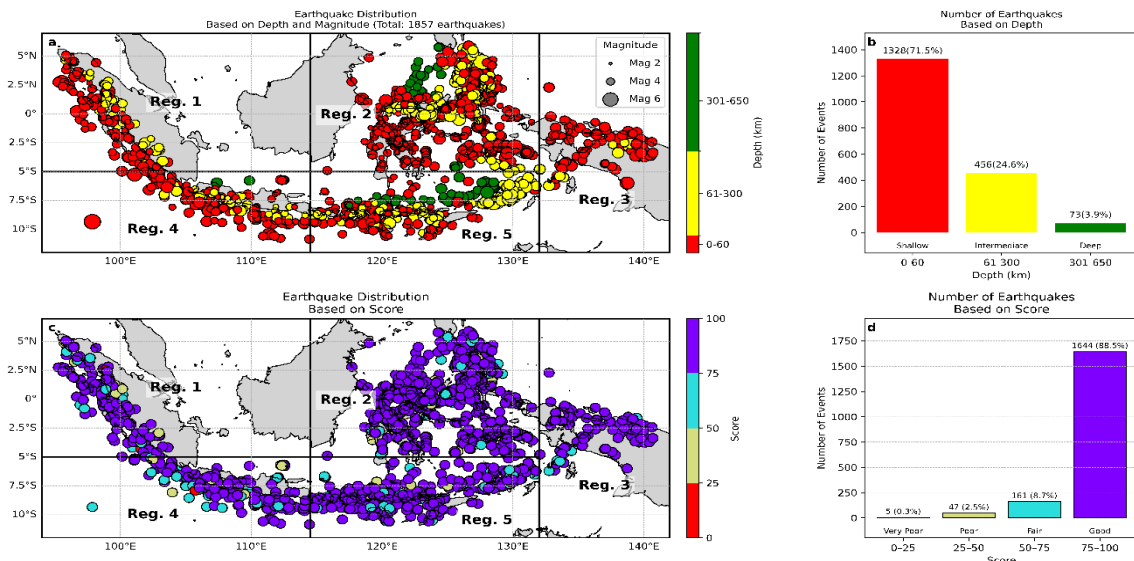


Figure 4. Automatic picking: (a) earthquake distribution based on depth and magnitude, (b) number of earthquakes based on depth, (c) earthquake distribution based on score, and (d) number of earthquakes based on score.

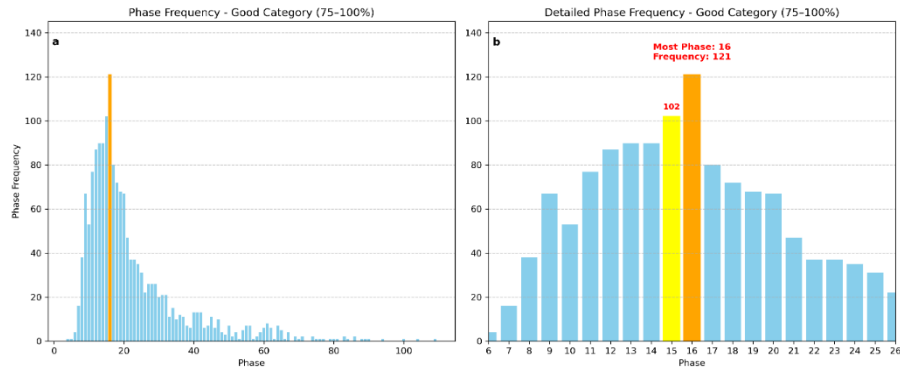


Figure 5. Automatic picking: (a) phase frequency – good category, and b) details

Based on Figures 5a–5b, it can be seen that most of the phases in the good category (score 75–100) are phases with a relatively low number of phases. This condition occurs because, in less than 3 minutes, the number of phases recorded is still small. This is due to the limited distribution of seismic stations in Indonesia, which limits the process of quickly recording earthquake phases.

In addition, the number of recorded phases is also influenced by the magnitude and depth of the earthquake. Earthquakes with larger magnitudes and shallower depths tend to produce more phases because more stations can record them. The phase that appears most frequently in the good category is phase 16, with 121 occurrences. This is followed by phase 15 with 102 occurrences.

Comparison of Automatic Picking (Region 1).

Based on Figures 6a–6b, the distribution of earthquake events in Region 1 (Sumatra Island and western Kalimantan) detected by automatic picking in less than 3 minutes shows a total of 172 earthquake events. Of these, shallow earthquakes (depth 0–60 km) dominate with 135 events (79.1%), followed by

intermediate earthquakes (60–300 km) with 36 events (20.9%). There are no deep earthquakes (300–650 km) in this region.

Specifically in western Kalimantan, no earthquake events were recorded. This is due to the region's location being far from the tectonic plate boundary [13]. Conversely, earthquakes frequently occur in the western part of Sumatra Island. This island has a high earthquake risk due to the collision between the Indo-Australian Plate and the Eurasian Plate west of Sumatra. The interaction between these two plates causes the formation of faults on the seabed and creates a subduction zone, which is the boundary between the subducting plates [14].

Meanwhile, based on Figures 6c–6d, the distribution of earthquake picking quality is dominated by the “good” category with a score of 75–100, covering 145 events (84.3%). Earthquakes with “fair” quality (scores of 50–75) accounted for 18 events (10.5%), while the ‘poor’ category (scores of 25–50) had 7 events (4.1%). The “very poor” category (scores of 0–25) was only recorded in 2 events (1.2%).

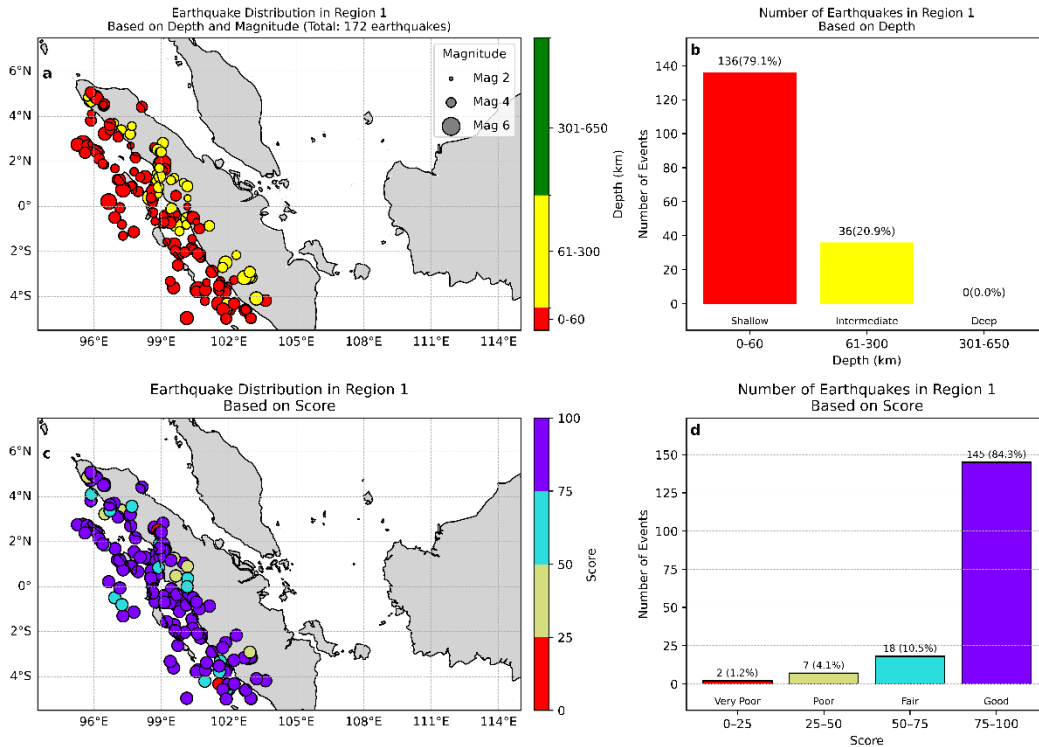


Figure 6 automatic picking: (a) earthquake distribution in region 1 based on depth and magnitude, (b) number of earthquakes in region 1 based on depth, (c) earthquake distribution in region 1 based on score, and (d) number of earthquakes in region 1 based on score.

Based on Figures 7a–7b, there were two earthquakes that fell into the very poor picking quality category (score 0–25). The first event was an earthquake with Event ID bmg2024kcvb, which had an initial magnitude of 5.15 and a depth of 15 km. This earthquake occurred on May 3, 2024, at 20:17:52 UTC and was analyzed using 17 seismic phases.

The magnitude difference between this earthquake and the final result is 1.19, with the initial value being greater. This difference falls into the very poor category. The origin time was recorded 73 seconds earlier than the final result, and it also falls into the very poor category. The RMS error of 2.22 seconds is considered acceptable, while the azimuth gap of 188° remains in the poor category. The difference in the earthquake's epicenter position reached 777 km, which is very large and falls into the very poor category. Additionally, the difference in depth reached 323 km, causing a change in classification from a deep earthquake to a shallow earthquake, and

it falls into the very poor category. Overall, the final score for this earthquake is 17, indicating very poor picking quality.

The second event was an earthquake with Event ID bmg2024omij, which had an initial magnitude of 4.4 and a depth of 135 km. This earthquake occurred on July 24, 2024, at 23:22:08 UTC, and was analyzed with 25 phases. The magnitude difference of 0.77 (initial value is larger) falls into the poor category, while the origin time difference of 28 seconds earlier also falls into the poor category. The RMS error of this earthquake is 1.2 seconds, still in the acceptable category, but the azimuth gap of 291° is very poor. The epicenter position difference of 443 km falls into the very poor category, as does the depth difference of 125 km, which changes the classification from shallow to intermediate. The final score for this earthquake is 25, which is the lower limit of the very poor category.

Details of the Lowest Scores in Region 1

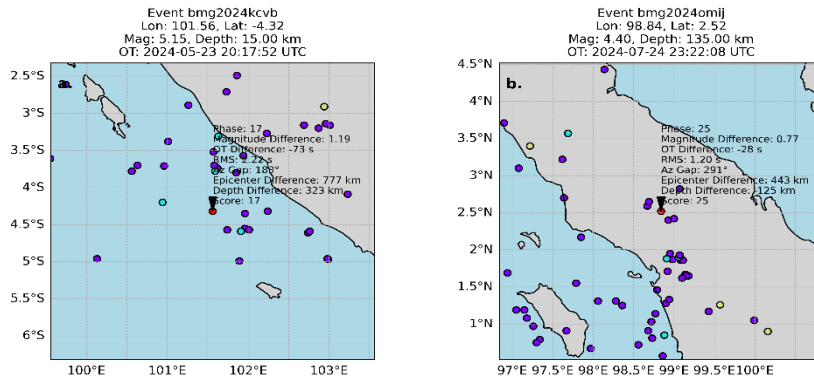


Figure 7 Automatic picking: details of the lowest scores in region 1 (a) event bmg2024kcvb (b) event bmg2024omij

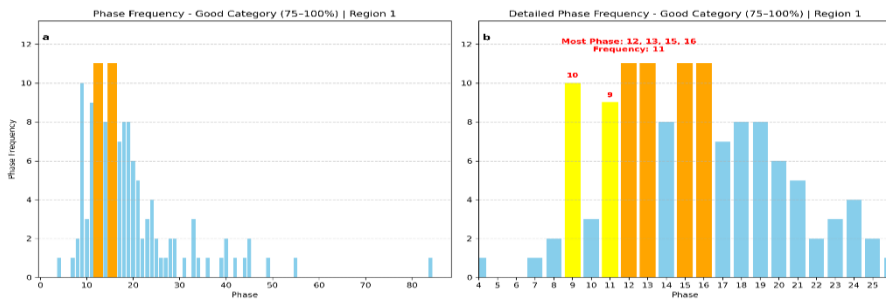


Figure 8 Automatic picking: (a) phase frequency – good category in region 1, and b) details

Based on Figures 8a–8b, most phases in the “good” quality category (score 75–100) are phases with a relatively low number of phases. This indicates that good picking quality does not always require a large number of phases. The phases most frequently appearing in the good category are phases 12, 13, 15, and 16, each with 11 occurrences. These are followed by phase 9 with 10 occurrences and phase 11 with 9 occurrences. From this pattern, it can be concluded that the minimum number of phases required for automatic picking results to approach the final results in Region 1 is phase 9.

Comparison of Automatic Picking (region 2). Based on Figures 9a–9b, there were 969 earthquake events in Region 2 (Sulawesi Island, Maluku, and eastern Kalimantan) detected by automatic picking in less than 3 minutes. Of these, shallow earthquakes with depths of 0–60 km dominated, accounting for 743 events (76.7%). Medium-depth earthquakes (depth 60–300 km) accounted for 201 events (20.7%), while deep earthquakes (depth 300–650 km) numbered 25 events (2.6%).

In the eastern part of Kalimantan, earthquake activity is very rare. This is due to the region's location, which is far from the boundaries of tectonic plates. Conversely, Sulawesi Island and Maluku are tectonically active regions. Geologically, Sulawesi Island is located at the meeting point of four major

tectonic plates, namely the Eurasia Plate, the Indo-Australian Plate, the Pacific Plate, and the Philippine Sea Plate [15].

The Maluku Islands are known to have a high level of earthquake and tsunami vulnerability [16]. This is due to the presence of two double subduction zones in the region. The first subduction zone originates from the Pacific Plate through the Halmahera Arc, which pushes westward, while the second subduction zone originates from the Eurasian Plate through the Sangihe Arc, which pushes eastward. In the southern part of this region, there is also the Sorong Fault, which plays an important role in tectonic activity. These two opposing subduction zones form an asymmetrical double-dip system. The pressure from the Philippine Sea Plate in the Halmahera zone and the eastward thrust of the Sangihe Plate reinforce the tectonic complexity of the Maluku region [17].

Meanwhile, based on Figures 9c–9d, the quality of earthquake picking in Region 2 shows that the majority are classified as “good” with a score of 75–100, covering 880 events (90.8%). Earthquakes with “fair” quality (scores of 50–75) accounted for 71 events (7.3%), while the “poor” category (scores of 25–50) was only found in 16 events (1.7%). The “very poor” category (scores of 0–25) is extremely rare, with only 2 events (0.2%) recorded.

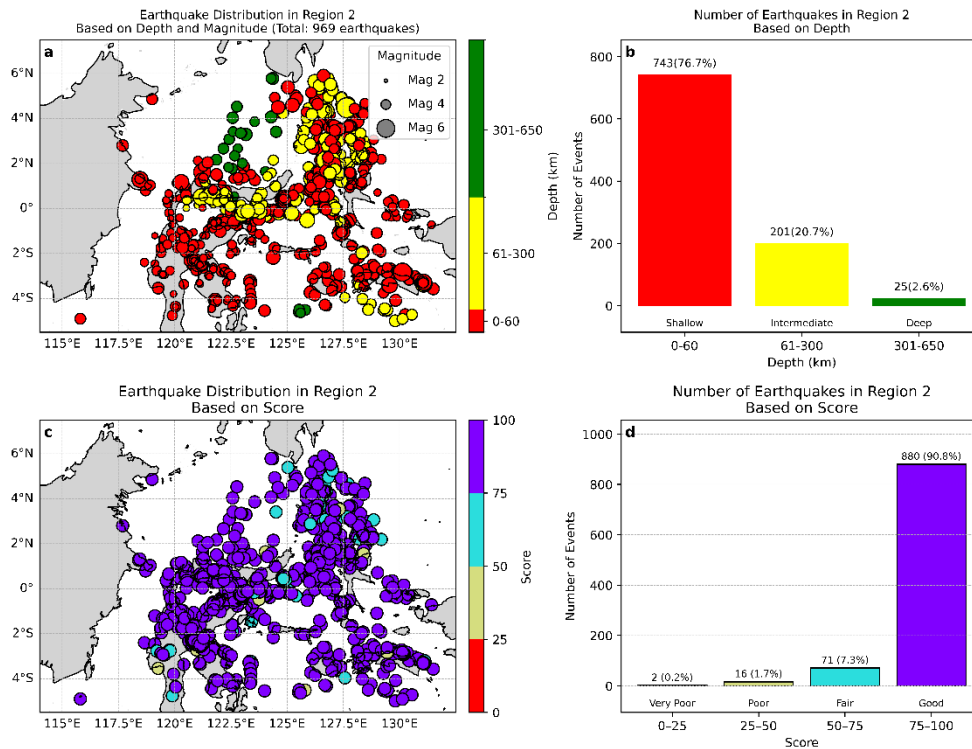


Figure 9 Automatic picking: (a) earthquake distribution in region 2 based on depth and magnitude, (b) number of earthquakes in region 2 based on depth, (c) earthquake distribution in region 2 based on score, and (d) number of earthquakes in region 2 based on score.

Based on Figures 10a–10b, two earthquake events were classified within the very poor picking quality category (score range: 0–25). The first event, identified by event ID bmg2024svqu, had an initial magnitude of 5.21 and a focal depth of 10 km. This earthquake occurred on 24 September 2024 at 23:59:32 UTC, with a total of ten seismic phases utilized in the picking process. The magnitude discrepancy between the initial and final solutions was 1.85, with the initial value being higher. This difference is categorized as very poor in terms of magnitude consistency. Furthermore, the origin time exhibited a deviation of 58 seconds earlier than the final solution, which also falls within the very poor quality classification.

Additionally, the RMS error value reached 3.32 seconds, which is classified as poor. The azimuth gap of 188° is also classified as poor. The difference in epicenter location is highly significant, at 460 km, placing it in the very poor category. The depth difference reached 280 km, causing a change in

classification from a moderate earthquake to a shallow earthquake. Overall, this earthquake received a final score of only 10, indicating very poor picking quality.

The second event was an earthquake with event ID bmg2024meed, which had an initial magnitude of 4.86 and a depth of 5 km. This earthquake occurred on June 22, 2024, at 01:05:16 UTC, with 15 phases used in picking. The magnitude difference was 1.17 (the initial value was larger), and the origin time difference was 67 seconds faster, both of which fall into the very poor category. The RMS error reached 1.88 seconds and was classified as fair, but the azimuth gap of 268° remained in the poor category. The epicenter difference reached 526 km, which is classified as very poor. The depth difference was also very large, at 508 km, changing the classification from a deep earthquake to a shallow one. The final score for this earthquake is 15, which is exactly at the lower boundary of the very poor category.

Details of the Lowest Scores in Region 2

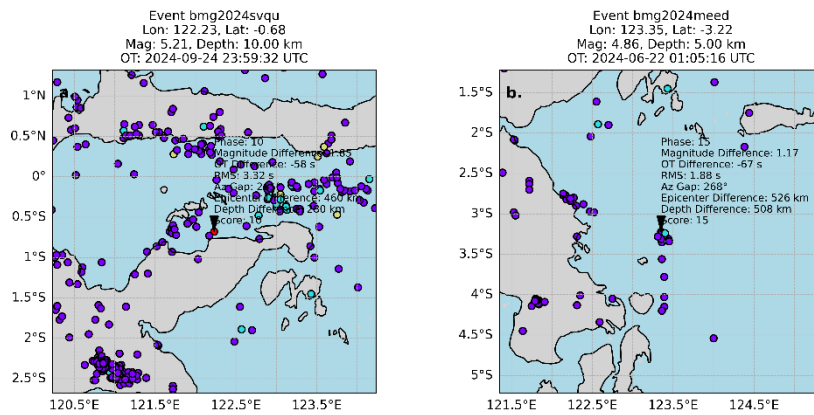


Figure 10 Automatic picking: details of the lowest scores in region 2 (a) event bmg2024svqu (b) event bmg2024meed

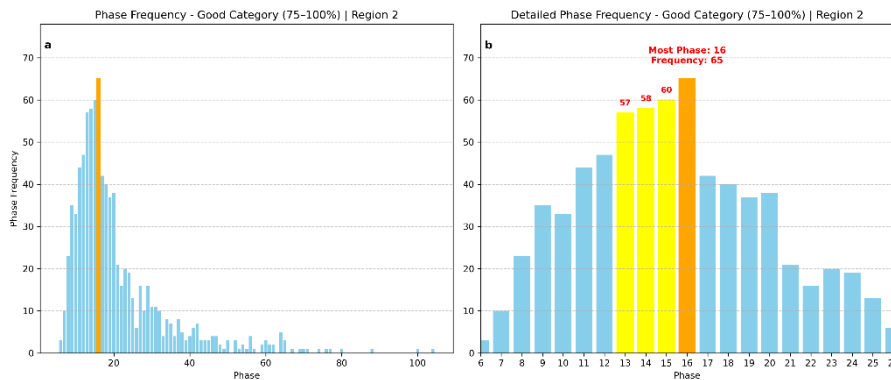


Figure 11 Automatic picking : (a) phase frequency – good category in region 2, and b) details

Based on Figures 11a–11b, most phases classified as “good” quality (scores 75–100) are relatively low in number. The phase that appears most frequently in the good category is phase 16, which occurred 65 times. Next, phase 15 appears 60 times, followed by phase 14 with 58 occurrences, and phase 13 with 57 occurrences. From this pattern, it can be concluded that the minimum number of phases required for automatic picking results to approach the final results in Region 2 is starting from phase 13.

Comparison of Automatic Picking (Region 3).

Based on Figures 12a–12b, there were 104 earthquake events in Region 3 (Papua Island and surrounding areas) that were successfully detected by automatic picking within less than 3 minutes. Of these, shallow earthquakes with depths of 0–60 km

dominated, accounting for 93 events (89.4%). There were 11 medium earthquakes (depth 60–300 km) (10.6%), while no deep earthquakes (depth 300–650 km) were detected. The number of earthquakes successfully detected by automatic picking in the Papua region is relatively low compared to other regions. This is likely due to the limited distribution of seismic sensors in the area.

Meanwhile, based on Figures 12c–12d, the quality of earthquake picking in Region 3 shows that the majority are in the “good” category with a score of 75–100, covering 95 events (91.3%). Earthquakes with “fair” quality (score 50–75) were recorded in 9 events (8.7%). No events with “poor” quality (score 25–50) or “very poor” quality (score 0–25) were found.

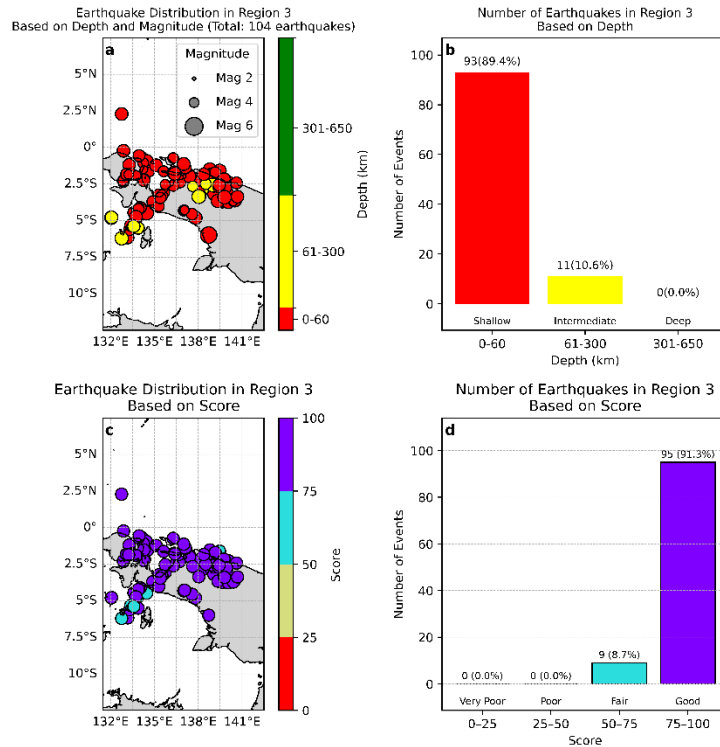


Figure 12 Automatic picking: (a) earthquake distribution in region 3 based on depth and magnitude, (b) number of earthquakes in region 3 based on depth, (c) earthquake distribution in region 3 based on score, and (d) number of earthquakes in region 3 based on score.

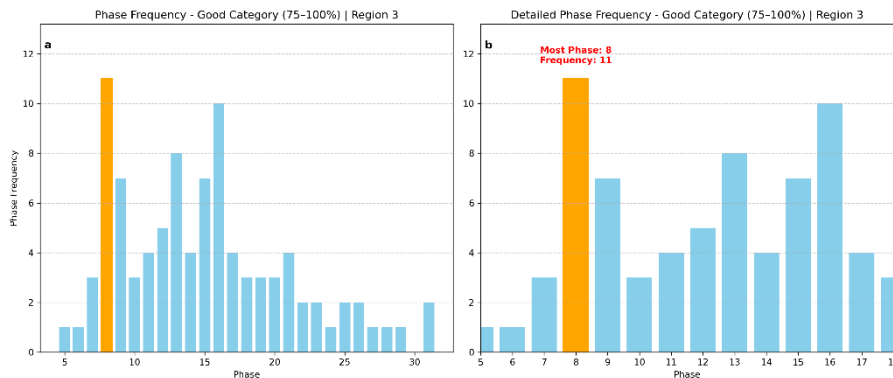


Figure 13 Automatic picking: (a) phase frequency – good category in region 3, and (b) details

Based on Figures 13a–13b, most phases in the “good” quality category (with scores of 75–100) are fairly evenly distributed across phases 5 to 31. However, the dominant phases are those below phase 16. The phase that appears most frequently in the “good” category is phase 8, with a total of 11 occurrences. From this pattern, it can be concluded that the minimum number of phases required for the automatic picking results to approach the final results in Region 3 is starting from phase 8.

Comparison of Automatic Picking (Region 4). Based on Figures 13a–13b, there were 225 earthquake events in Region 4 (Java Island and surrounding areas) detected by automatic picking within less than 3 minutes. Of these, shallow earthquakes with depths of 0–60 km dominated, accounting for 195 events (86.7%). Medium-depth

earthquakes (depth 60–300 km) accounted for 28 events (12.4%), while deep-focus earthquakes (depth 300–650 km) numbered 2 events (0.9%).

Earthquakes are distributed across the southern part of Java Island, influenced by the presence of a subduction zone at the boundary of the Indo-Australian and Eurasian plates. This plate boundary forms a subduction zone extending along the southern coast of Java [18], [19]. Additionally, Java Island is crossed by several active faults, such as the Opak Fault, Lembang Fault, and Cimandiri Fault, which also contribute to seismic activity. In the northern part of Java Island, earthquakes have also been recorded around the Bawean Island area. The presence of subduction zones and active fault lines causes deformation of the Earth's crust. Seismic activity

along these two geological structures is a potential source of tectonic earthquakes [20]

Meanwhile, based on Figures 14c–14d, the quality of earthquake picking in Region 4 shows that the majority falls into the “good” category with a score of 75–100, covering 182 events (80.9%). Earthquakes with “fair” quality (scores of 50–75) account for 30 events (13.3%), while the “poor” category (scores of 25–50) is only found in 12 events (5.3%). The “very poor” category (scores 0–25) is extremely rare, with only 1 event (0.4%) recorded.

Based on Figure 15, there was one earthquake event that fell into the very poor picking quality category (score 0–25). The earthquake with event ID bmg2025fukn had an initial magnitude of 4.62 and a depth of 22 km. This earthquake occurred on March 24, 2024, at 07:43:21 UTC, with 21 seismic phases

used in the picking process. The magnitude difference between the initial and final results is 1.23, with the initial value being greater. This difference falls into the very poor category. The origin time is recorded as 28 seconds slower than the final result, which is also classified as poor.

Additionally, the RMS error value reached 2.53 seconds, which is classified as poor. The azimuth gap of 202° is also classified as poor. The difference in epicenter location is very significant, at 469 km, placing it in the very poor category. The depth difference reached 190 km, causing a change in classification from a moderate earthquake to a shallow earthquake. Overall, this earthquake received a final score of only 21, indicating very poor picking quality.

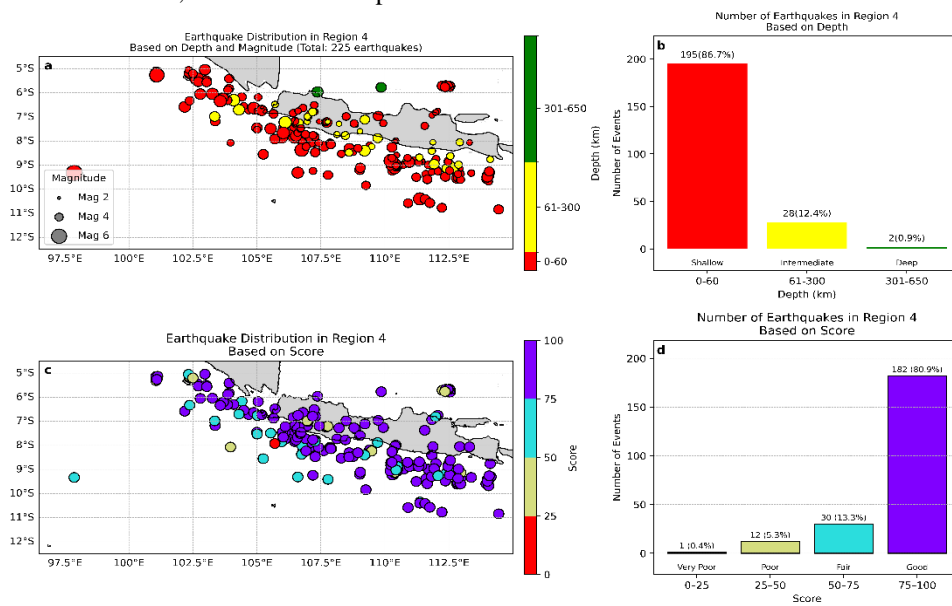


Figure 14 Automatic picking: (a) earthquake distribution in region 4 based on depth and magnitude, (b) number of earthquakes in region 4 based on depth, (c) earthquake distribution in region 4 based on score, and (d) number of earthquakes in region 4 based on score

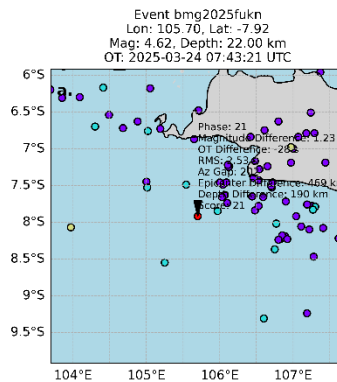


Figure 15 Automatic picking: details of the lowest scores in region 4 event bmg2025fukn

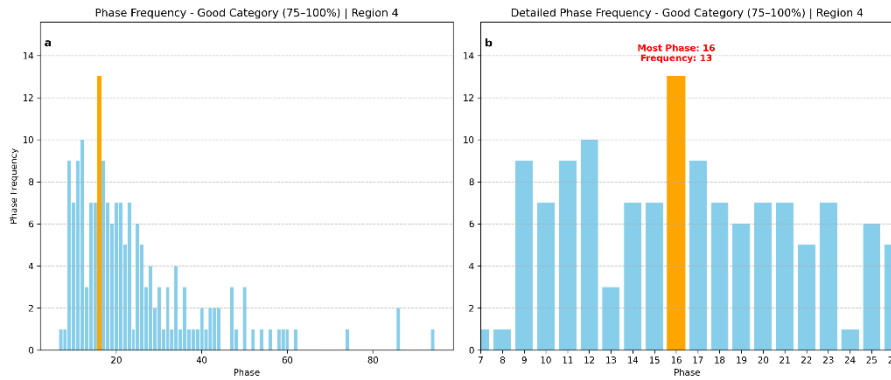


Figure 16 Automatic picking: (a) phase frequency – good category in region 4, and b) details

Based on Figures 16a–16b, most phases in the “good” quality category (score 75–100) are phases with relatively low numbers. The phase that appears most frequently in the good category is phase 16, which was recorded 13 times. From this pattern, it can be concluded that the minimum number of phases required for the automatic picking results to approach the final results in Region 4 is starting from phase 16.

Comparison of Automatic Picking (Region 5).

Based on Figures 17a–17b, there were 387 earthquake events in Region 5 (Bali Island, Lombok, Nusa Tenggara, and surrounding areas) detected by automatic picking within less than 3 minutes. Of these, shallow earthquakes with depths of 0–60 km accounted for 161 events (41.6%). Intermediate-depth earthquakes (60–300 km) totaled 180 events (46.5%), while deep earthquakes (300–650 km) numbered 46 events (11.9%).

Moderate earthquakes dominate the Banda Sea region (east), accompanied by numerous deep earthquakes in the area. This is due to the presence of a subduction zone resulting from the interaction between the Australian Plate and the Pacific Plate in the Banda Sea [21]. The complexity of the regional geology is a dominant factor that triggers tectonic earthquakes with tsunami potential [22]. The subduction zone in this region is known as the Banda Arc, which has a geometry shaped like a 180° open basin towards the west [23]. In addition, the subduction zone in the southern part also plays a role in the occurrence of earthquakes. Geologically, the island of Bali is located at the meeting point of three tectonic plates, namely the Eurasian Plate, the Pacific Plate, and the

Indo-Australian Plate. These three plates move at different speeds and in different directions, causing shifts at the plate boundaries in the southern part of Java, including Bali and Nusa Tenggara [24]. The strategic location above the Eurasian and Indo-Australian continental plates makes this region highly vulnerable to earthquake risks [25].

In the Bali and Nusa Tenggara regions, shallow and moderate earthquakes also occur frequently. One of the triggers is the Flores Back Arc Thrust Fault, better known as the Flores Thrust Fault [26]. This fault is an active submarine fault that dips or rises toward the south at a low to moderate angle, located north of the islands in the Sunda Arc, including Bali, Lombok, Sumbawa, Flores, Sumba, Rote, and Timor [27]. The Flores Thrust Fault was formed due to the reverse thrust of the Eurasian Plate against the Indo-Australian Plate, with a displacement rate of approximately 5.6–6.0 mm per year [28]. The activity of this fault often serves as the source of earthquakes in the northern part of Bali Island, West Nusa Tenggara, and East Nusa Tenggara.

Meanwhile, based on Figures 17c–17d, the quality of earthquake picking in Region 4 shows that the majority are classified as “good” with a score of 75–100, covering 342 events (88.4%). Earthquakes with “fair” quality (scores of 50–75) accounted for 33 events (8.5%), while the ‘poor’ category (scores of 25–50) was found in only 12 events (3.1%). No events were recorded in the “very poor” category (scores of 0–25).

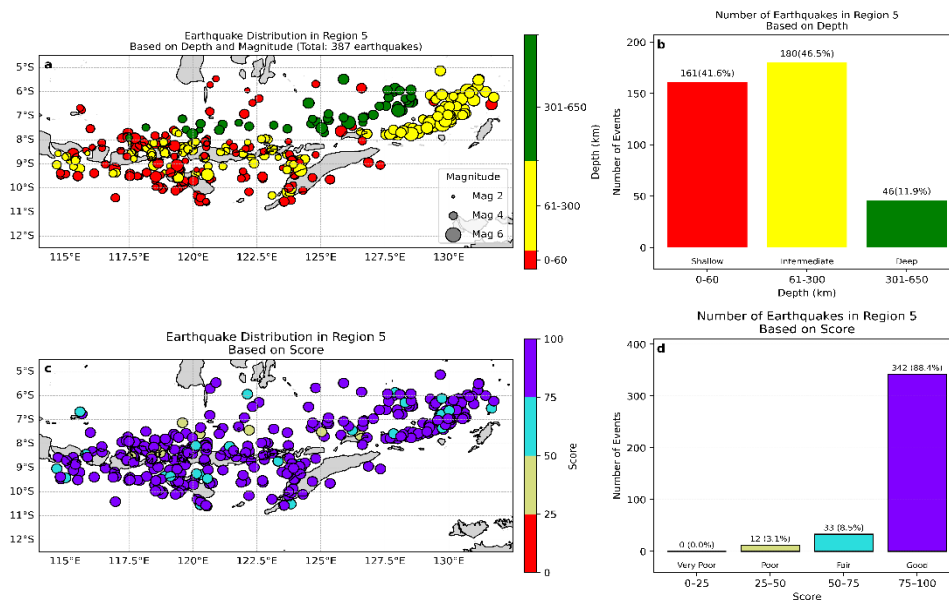


Figure 17 Automatic picking: (a) earthquake distribution in region 5 based on depth and magnitude, (b) number of earthquakes in region 5 based on depth, (c) earthquake distribution in region 5 based on score, and (d) number of earthquakes in region 5 based on score.

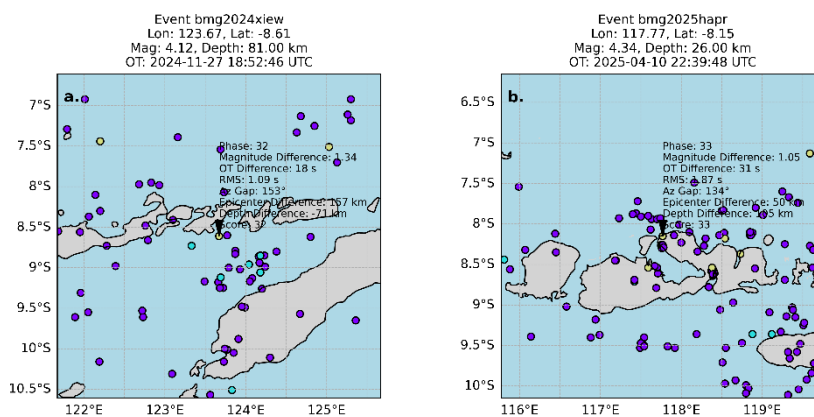


Figure 18 Automatic picking: details of the lowest scores in region 5 (a) event bmg2024xiew (b) event bmg2025hapr

Based on Figures 18a–18b, there were two earthquakes that fell into the poor picking quality category (score 25–50). The first event was an earthquake with event ID bmg2024xiew, which had a magnitude of 4.12 and a depth of 81 km. This earthquake occurred on November 27, 2024, at 18:52:46 UTC, with 32 phases used. The magnitude difference was recorded as 1.34, greater than the final result, falling into the very poor category. The origin time was recorded as 18 seconds slower than the final result, falling into the fair category. The RMS value of 1.09 seconds falls into the good category, while the azimuth gap of 153° falls into the fair category. The epicenter difference reached 157 km, categorized as very poor. The depth also changed from shallow to intermediate, being 71 km shallower than the final result, thus falling into the very poor category. The

final score for this earthquake is 32, categorized as poor.

The second event was an earthquake with event ID bmg2025hapr, which had a magnitude of 4.34 and a depth of 26 km. This earthquake occurred on April 10, 2025, at 22:39:48 UTC, with 33 phases used. The magnitude difference was recorded as 1.05 greater than the final result. The original time was recorded as 31 seconds slower than the final result. The RMS value of 1.87 seconds falls into the adequate category, and the azimuth gap of 134° also falls into the adequate category. The epicenter difference reached 50 km, which is categorized as adequate. The depth changed from the intermediate classification to shallow, being 105 km deeper than the final result, falling into the poor category. The final score for this earthquake is 33, categorized as poor.

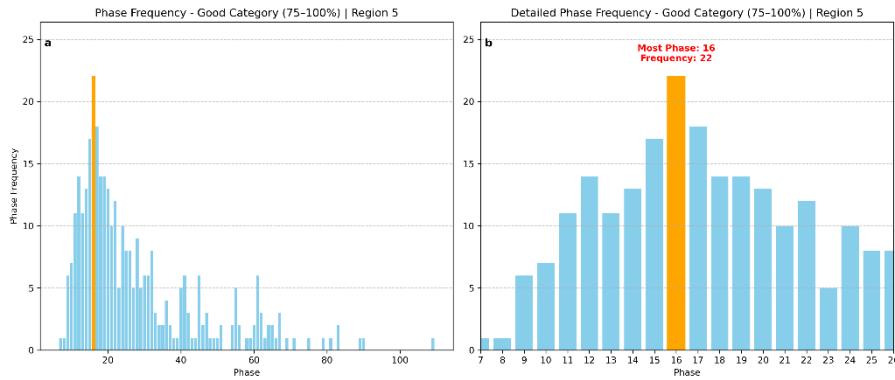


Figure 19 Automatic picking: (a) phase frequency – good category in region 5, and b) details

Based on Figures 19a–19b, most phases included in the “good” quality category (score 75–100) are phases with relatively low numbers. The phase that appears most frequently in the good category is phase 16, which was recorded 22 times. From this pattern, it can be concluded that the minimum number of phases required for the automatic picking results to approach the final results in Region 5 is from phase 16 onwards.

Manual Picking Comparison. Based on Figures 20a–20b, the distribution of earthquakes in Indonesia with manual picking of S waves less than 3 minutes (<3 minutes) was recorded at 327 events, or only 11.7% of the total earthquakes. This number is much smaller than the previous automatic picking, because manual picking is done by operators, and operators do not perform picking quickly. Of these, shallow earthquakes (0–60 km) dominate with 257 events

(78.6%), followed by intermediate earthquakes (60–300 km) with 67 events (20.5%), and deep earthquakes (300–650 km) with 3 events (0.9%).

Shallow and intermediate earthquakes are evenly distributed across most of Indonesia, reflecting widespread seismic activity. Meanwhile, deep earthquakes are generally concentrated in the northern regions of Bali, West Nusa Tenggara (NTB), East Nusa Tenggara (NTT), and northern Sulawesi. The Kalimantan region does not show significant seismic activity. Meanwhile, based on Figures 20c–20d, the distribution of earthquakes based on picking quality scores is dominated by the good category (scores 75–100) with 317 events (96.9%). The fair category (score 50–75) includes 9 earthquakes (2.8%), followed by poor (25–50) with 1 earthquake (0.3%), and very poor (0–25) with no earthquake events.

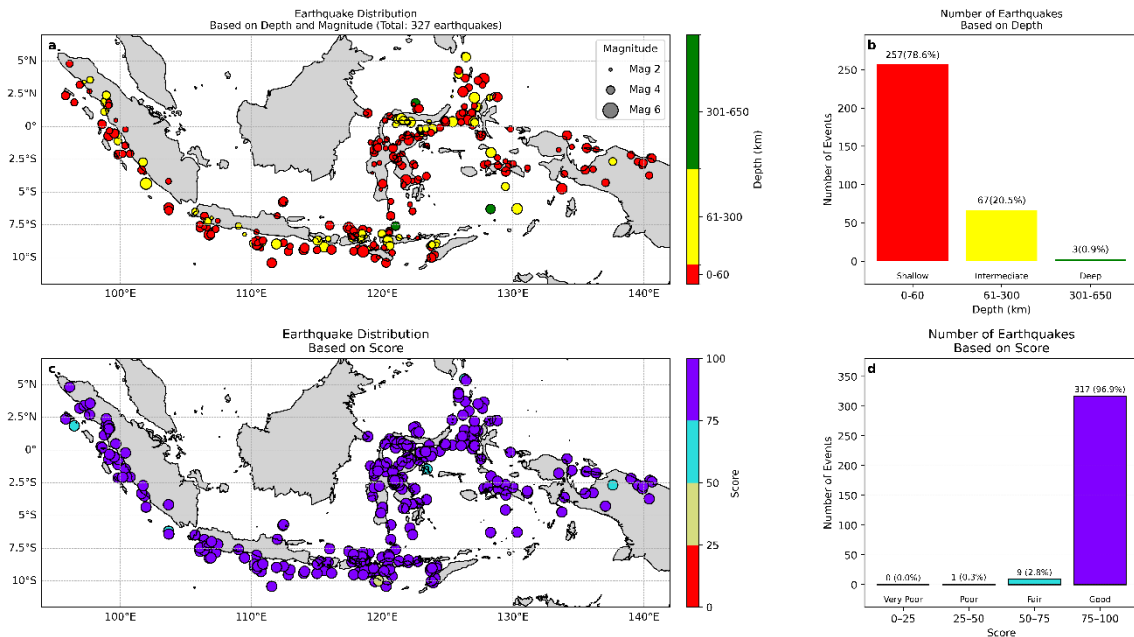


Figure 20 Manual picking: (a) earthquake distribution based on depth and magnitude, (b) number of earthquakes based on depth, (c) earthquake distribution based on score, and (d) number of earthquakes based on score.

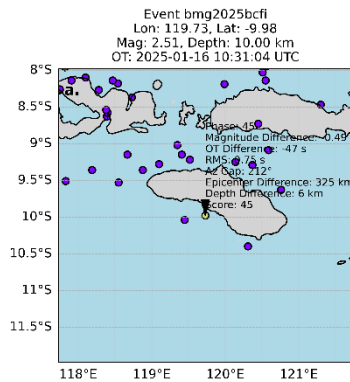


Figure 21 Manual picking: details of the lowest score event bmg2025bcfi

Based on Figure 21, there was one earthquake event that fell into the poor picking quality category (score 25–50). This earthquake had an event ID of bmg2025bcfi, with a magnitude of 2.51 and a depth of 10 km. The number of phases used in the analysis was 45. The magnitude difference of this earthquake is 0.49, which is greater than the final result, thus falling into the adequate category. The origin time is recorded as 47 seconds earlier than the final result and falls into the very poor category. The azimuth gap value of 212° is categorized as poor. For the epicenter difference, the distance reaches 325 km, which falls into the very poor category. Meanwhile, the depth difference is only 6 km deeper than the final result, which is categorized as very good. Based on all these parameters, the final score for this earthquake is 45, placing it in the poor quality category.

Discussion. Before analyzing the results, it is important to reiterate the framework of this study. As stated in the Introduction, this study conducts two separate evaluations (automatic vs. final, and fast-manual vs. final), not a direct comparison between the automatic and fast-manual methods. The objective is to independently validate the baseline performance of the current automatic system and the fast manual protocol. The results of these two evaluations are therefore presented as independent findings.

Based on previous results, the number of earthquake events that can be processed by automatic picking in less than three minutes (<3 minutes) is much higher than manual picking in the same time frame. Automatic picking successfully recorded 1,857 earthquakes, while manual picking only recorded 327 earthquakes. In terms of quality, the number of data points with a good category score (75–100) in automatic picking reached 1,644 earthquakes (88.5%), while manual picking recorded 317 earthquakes (96.9%). The higher percentage in manual picking is understandable since the process is directly performed by an operator. However, for the rapid dissemination of earthquake information, especially within three minutes, automatic picking is more suitable. In addition to being able to process

more data, the results are also quite close to the final results.

Each parameter shows a poor score, whether it be the magnitude difference, origin time difference, RMS, azimuth gap, epicenter difference, or depth difference. One of the causes of the low score is the large azimuth gap value. Practically, a large gap (e.g., $>180^\circ$) means most stations are on one side of the epicenter, which severely degrades location accuracy and can be the difference between a correct offshore (tsunami potential) or incorrect onshore location. This condition can occur because the distribution of earthquake sensors in Indonesia is not yet evenly distributed, as clearly shown in Figure 2, especially in border areas such as the Sumatra and Java subduction zones.

One solution to address the azimuth gap problem is the implementation of an ocean-bottom sensor network (for example, the DONET (Dense Oceanfloor Network system for Earthquakes and Tsunamis) system). DONET is a dense ocean floor sensor network for monitoring earthquakes and tsunamis [29]. This system is currently in use in the Nankai Trough, Japan, which is a region prone to megathrust earthquakes [30]. The equipment is capable of detecting various seafloor movements, ranging from slow crustal deformation to rapid shaking caused by earthquakes. The concept of an ocean-bottom sensor network is presented here as a potential long-term solution, as it is specifically designed to address the large azimuth gaps in subduction zones, a key problem identified in our data.

A high RMS factor may occur due to discrepancies between picking results and theoretical results. An RMS value > 1.0 s, for example, indicates a poor fit to the velocity model, which directly impacts the reliability of the calculated depth and origin time—critical parameters for hazard assessment. These theoretical results are based on P-wave and S-wave velocity models beneath the Earth's surface. Differences in epicenter, depth, and origin time (time of earthquake occurrence) can also be influenced by this velocity model. One important factor in improving the accuracy of epicenter location and depth is the availability of seismic wave velocity models at the local or regional scale with a high degree of precision [31].

Differences in magnitude results can also arise due to differences in P-wave picking between the initial data in the automatic picking system and the final data. Automatic picking typically uses the STA/LTA method, which only detects P-waves. This condition poses a challenge because the magnitude calculation may not match the final data. A solution that can be used is to apply machine learning-based automatic picking, which is capable of automatically picking not only P-waves but also S-waves [32]. As shown in

Figure 22, the automatic picking method using machine learning has proven to be more effective than the STA/LTA method.

Based on the research results, it is known that the minimum number of phases required to achieve good automatic picking quality (score 75–100) varies across regions. Nationally, the phase most frequently appearing in the good category is phase 16 with 121 occurrences, followed by phase 15 with 102 occurrences. This indicates that, on a national scale, the minimum phase required to achieve the good category is phase 15. For Region 1, the phases most frequently appearing in the good category are phases 12, 13, 15, and 16, each with 11 occurrences. This is followed by phase 9 with 10 occurrences and phase 11 with 9 occurrences. From this pattern, it can be concluded that the minimum phase required to achieve the good category in Region 1 is phase 9.

In Region 2, the most frequently occurring phase in the good category is phase 16 with 65 occurrences, followed by phase 15 (60 occurrences), phase 14 (58 occurrences), and phase 13 (57 occurrences). Thus, the minimum phase required to achieve the good category in Region 2 is phase 13. In Region 3, the phase that most frequently appeared in the good category was phase 8 with 11 occurrences. This indicates that the minimum phase required in Region 3 to obtain a good category is phase 8.

For Region 4, the phase that appears most frequently in the good category is phase 16, with 13 occurrences. This means that the minimum phase required in Region 4 is phase 16. Meanwhile, in Region 5, phase 16 is also the most frequently occurring phase in the good category, with 22 occurrences. This means that the minimum phase required in Region 5 is phase 16. Interestingly, in Regions 4 and 5, these results are considered unusual. As seen in Figure 2, these regions (Java, Bali, NT) indeed have a dense distribution of stations *on land*. However, for earthquakes occurring offshore in the southern subduction zone, this station geometry results in a persistently large azimuth gap (as most stations are on one side of the epicenter). This explains why a higher number of phases (Phase 16) is still required to achieve a 'good' quality automatic solution in these areas, despite the high station density.

In the manual picking comparison, it was found that the amount of data below 3 minutes (<3 minutes) was much less than the automatic and final data. However, for the good category score (75–100), the percentage of manual picking supplemented with S waves was higher than automatic picking, namely 96.9% compared to 88.5%. These results are in line with previous research stating that the determination of earthquake hypocenters is greatly influenced by the time difference between the arrival of P and S waves [10]. In addition, S-waves are also useful in determining earthquake depth [11] and can even

influence the determination of other earthquake parameters.

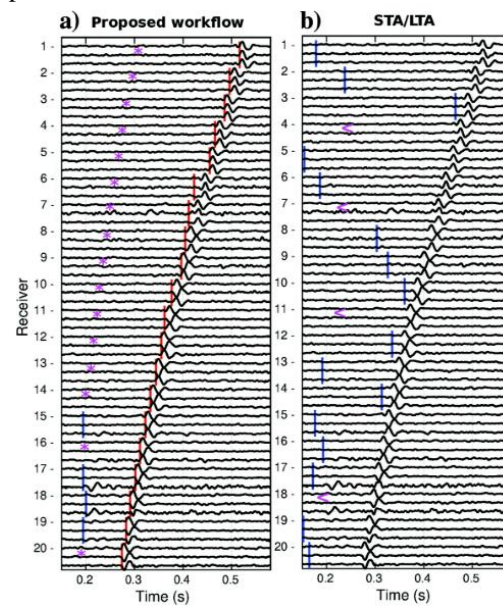


Figure 22 (a) Machine Learning picks, (b) STA/LTA picks [32]

4. Conclusion

Based on the research results, the number of earthquake events that can be processed by automatic picking in less than three minutes (<3 minutes) is much higher than manual picking in the same time frame. Automatic picking successfully recorded 1,857 (66.6%) earthquakes, while manual picking only recorded 327 (11.7%) earthquakes. In terms of quality, the number of data points with a good category score (75–100) in automatic picking reached 1,644 earthquakes (88.5%), while manual picking recorded 317 earthquakes (96.9%). The higher percentage in manual picking is understandable since the process is directly performed by the operator. However, for the need to disseminate earthquake information quickly, especially within three minutes, automatic picking is more suitable. In addition to processing more data, the results are also quite close to the final results. Nationally, the minimum phase required for automatic picking to achieve a good rating is phase 15. When viewed by region, the minimum phase required to achieve a good rating is as follows:

1. Region 1: phase 9
2. Region 2: phase 13
3. Region 3: phase 8
4. Region 4: phase 16
5. Region 5: phase 16

Our findings strongly support a hybrid operational protocol, which represents a vital contribution to global best practices by demonstrating how a regional network can statistically balance the speed of automated alerts against the need for rapid, high-accuracy human validation. Automatic picking is

reliable enough for the initial rapid early warning (provided a sufficient number of phases are available), while fast manual picking remains critical for validating accuracy before final dissemination. In this way, both methods play complementary roles in earthquake monitoring.

To improve the accuracy of automatic sorting, several steps based on our findings can be taken. First, to address the large azimuth gap identified in our analysis, expand the sensor network to reduce the azimuth gap, especially in marine and border areas, for example, by implementing an ocean-bottom sensor network such as the DONET (Dense Oceanfloor Network System for Earthquakes and Tsunamis) system, such as in the Nankai Trough, Japan. Second, to improve theoretical travel times and address the RMS errors found, refine the P and S wave velocity models on a local and regional scale so that the results of determining the epicenter, depth, and time of origin are more accurate. Third, to automate the inclusion of S-waves, which our analysis proved is critical for achieving high accuracy, adopt machine learning technology in automatic sorting methods, which enables simultaneous detection of P and S waves, so that the calculation of magnitude, epicenter, depth, and time of origin is more accurate than conventional methods such as STA/LTA.

Acknowledgement

We would like to thank BMKG and STMKG for providing the data and facilities used in this study.

References

- [1] Y. Syafitri, B. Bahtiar, and L. A. Didik, "Analisis Pergeseran Lempeng Bumi Yang Meningkatkan Potensi Terjadinya Gempa Bumi Di Pulau Lombok," *Konstan - Jurnal Fisika Dan Pendidikan Fisika*, vol. 4, no. 2, pp. 139–146, 2020, doi: 10.20414/konstan.v4i2.43.
- [2] A. W. Sari, R. Jasruddin, and N. Ihsan, "Analisis rekahan gempa bumi dan gempa bumi susulan dengan menggunakan metode omori," *Jurnal Sains dan Pendidikan Fisika*, vol. 8, no. 3, pp. 263–268, 2012, [Online]. Available: <https://ojs.unm.ac.id/JSdPF/article/view/922>
- [3] H. Helmi, G. I. Marliyani, and S. Nur'aini, "Identifikasi Sesar Aktif di Pulau Bali dengan Menggunakan Data Pemetaan Geologi Permukaan dan Morfologi Tektonik," *Majalah Geografi Indonesia*, vol. 35, no. 1, p. 45, 2021, doi: 10.22146/mgi.61928.
- [4] Akmam, "Subduksi Lempeng Indo-Australia Pada Lempeng," *Jurnal Saintek*, vol. 3, no. 1, pp. 52–59, 2011.
- [5] A. Y. Baeda and F. Husain, "Kajian Potensi Tsunami Akibat Gempa Bumi Bawah Laut di Perairan Pulau Sulawesi," *Jurnal Teknik Sipil*, vol. 19, no. 1, p. 75, 2012, doi: 10.5614/jts.2012.19.1.7.
- [6] D. S. Farah, W. Raharjo, S. Prayoehdhie, D. Vermiratih, and Y. Hadi Perdana, "Penentuan Aftershock Gempabumi Yogyakarta Tanggal 6 Juni 2006 Dengan Menggunakan Metode Geiger," *Jurnal Stasiun Geofisika Sleman*, vol. 1, no. 1, pp. 24–28, 2023.
- [7] J. N. Williams, D. Eberhart-Phillips, S. Bourguignon, M. W. Stirling, and W. Oliver, "Deep and Clustered Microseismicity at the Edge of Southern New Zealand's Transpressive Plate Boundary," *Journal of Geophysical Research: Solid Earth*, vol. 130, no. 5, 2025, doi: 10.1029/2024JB030371.
- [8] G. Brenn, S. Shamsalsadati, C. Sippl, and M. Comoglu, "Automated Relocation of the Petermann Ranges Aftershock Sequence Automated Relocation of the Petermann Ranges Aftershock Sequence," *Australian Earthquake Engineering Society*, no. April, 2022.[9] Y. Vaezi and M. Van der Baan, "Comparison of the STA/LTA and power spectral density methods for microseismic event detection," *Geophysical Journal International*, vol. 203, no. 3, pp. 1896–1908, 2015, doi: 10.1093/gji/ggv419.
- [10] M. Singh and G. Rumpker, "Seismic gaps and intraplate seismicity around Rodrigues Ridge (Indian Ocean) from time domain array analysis," *Solid Earth*, vol. 11, no. 6, pp. 2557–2568, 2020, doi: 10.5194/se-11-2557-2020.
- [11] D. S. Dreger and D. V. Helmberger, "Determination of source parameters at regional distances with three- component sparse network data," *Journal of Geophysical Research*, vol. 98, no. B5, pp. 8107–8125, 1993, doi: 10.1029/93JB00023.
- [12] T. O. Hodson, "Root-mean-square error (RMSE) or mean absolute error (MAE): when to use them or not," *Geoscientific Model Development*, vol. 15, no. 14, pp. 5481–5487, 2022, doi: 10.5194/gmd-15-5481-2022.
- [13] D. Tjitradi, E. Eliatun, H. Khatimi, A. Karim, D. D. Lestari, and A. Tjitradi, "Desain Praktis Beban Gempa Dasar Untuk Bangunan Di Lahan Basah Kabupaten Banjar Kalimantan Selatan," *Borneo Engineering: Jurnal Teknik Sipil*, vol. 8, no. 2, pp. 212–226, 2024, [Online]. Available: <http://rsa.ciptakarya.pu.go.id/2021/>
- [14] K. Sakdiyah, "(LGCP) untuk Pemetaan Risiko Gempa Bumi di Sumatra," *Jurnal Sains dan Seni ITS*, vol. 9, no. 2, pp. 108–114, 2020.

- [15] G. Pasau and G. H. Tamuntuan, "Pengamatan Seismisitas Gempa Bumi Di Wilayah Pulau Sulawesi Menggunakan Perubahan Nilai a-b," *Jurnal Mipa Unsrat Online*, vol. 6, no. 1, pp. 31–35, 2017.
- [16] I. F. Jannah, Supardiyono, and Madlazim, "ANALISIS MODEL KECEPATAN LOKAL GELOMBANG PRIMER 1-D DAN KOREKSI STASIUN DI KEPULAUAN MALUKU" *Jurnal Fisika*, vol. 2, no. 2, pp. 1–5, 2012.
- [17] I. Septiani and D. Pujiastuti, "Analisis Seismisitas Wilayah Kepulauan Maluku Periode 1970-2019 dengan Menggunakan Metode Likelihood," *Jurnal Fisika Unand*, vol. 10, no. 4, pp. 461–466, 2021, doi: 10.25077/jfu.10.4.461-466.2021.
- [18] R. M. H. Dokht, Y. J. Gu, and M. D. Sacchi, "Migration Imaging of the Java Subduction Zones," *Journal of Geophysical Research Solid Earth*, vol. 123, no. 2, pp. 1540–1558, 2018, doi: 10.1002/2017JB014524.
- [19] S. J. Hutchings and W. D. Mooney, "The Seismicity of Indonesia and Tectonic Implications," *Geochemistry, Geophysics, Geosystems*, vol. 22, no. 9, pp. 1–42, 2021, doi: 10.1029/2021GC009812.
- [20] M. Fitria and T. Prastowo, "Seismisitas Jawa Timur Dan Potensi Bahaya Bencana Seismik Terkait," *Inovasi Fisika Indonesesia*, vol. 11, no. 1, pp. 17–27, 2022, doi: 10.26740/ifi.v11n1.p17-27.
- [21] S. A. R. Putri, M. N. Fahmi, and M. Madlazim, "Analisis Keakuratan Centroid Moment Tensor (Cmt) Pada Software Joko Tingkir Untuk Wilayah Laut Banda Menggunakan Metode Rmse Dan Sudut Kagan," *Inovasi Fisika Indonesia*, vol. 13, no. 3, pp. 7–17, 2024, doi: 10.26740/ifi.v13n3.p7-17.
- [22] J. Murjaya, "Seismotektonik Wilayah Indonesia Timur the Seismotectonic of Eastern Indonesia Region," *Buletin Meteorologi, Klimatologi, Dan Geofisika*, vol. 4, no. 3, pp. 14–22, 2023.
- [23] A. W. Baskara *et al.*, "Aftershock study of the 2019 Ambon earthquake using moment tensor inversion: identification of fault reactivation in northern Banda, Indonesia," *Earth, Planets, and Space*, vol. 75, no. 1, pp. 1–23, 2023, doi: 10.1186/s40623-023-01860-1.
- [24] R. I. Hielmy, "Tanah Maksimum Di Pulau Bali Comparison of Davenport , Milne , and Mcguirre Methods in Determining the Maximum Land Acceleration Value on the Island of Bali," *Buletin Meteorologi, Klimatologi, Dan Geofisika*, vol. 5, no. 5, pp. 9–16, 2024.
- [25] I. D. P. Dharyuuni *et al.*, "Dampak Gempa Regional di Pulau Bali, NTB dan NTT," *Prosiding Seminar Nasional Fisika Festival*, no. November 2019, pp. 71–76, 2019.
- [26] A. A. Bustari, "Kajian Seismisitas dan Energi Gempabumi Sesar Naik Busur Belakang Flores di Segmen Utara Pulau Lombok Berdasarkan Data Kegeempaan 2013-2023," *Jurnal Kolaboratif Sains*, vol. 7, no. 7, pp. 2268–2274, 2024, doi: 10.56338/jks.v7i7.5475.
- [27] X. Yang, S. C. Singh, and A. Tripathi, "Did the Flores backarc thrust rupture offshore during the 2018 Lombok earthquake sequence in Indonesia?," *Geophysical Journal International*, vol. 221, no. 2, pp. 758–768, 2020, doi: 10.1093/gji/ggaa018.
- [28] E. S. Ratuluhain, "Analisis Potensi Tsunami di Lombok Utara," *Jurnal Ilmu dan Teknologi Kelautan Tropis*, vol. 13, no. 1, pp. 113–126, 2021, doi: 10.29244/jitkt.v13i1.29336.
- [29] Y. Liu, M. Xue, Z. Guo, and A. Zhu, "Seismic Anisotropy Within the Subducting Northern Philippine Sea Plate, SW Japan, Using DONET Seafloor Observation Network," *Geophysical Research Letters*, vol. 49, no. 7, 2022, doi: 10.1029/2021GL096516.
- [30] K. Z. Nanjo, Y. Yamamoto, K. Ariyoshi, H. Horikawa, S. Yada, and N. Takahashi, "Earthquake detection capacity of the Dense Oceanfloor Network system for Earthquakes and Tsunamis (DONET)," *Journal of Seismology*, vol. 28, no. 3, pp. 787–810, 2024, doi: 10.1007/s10950-024-10219-2.
- [31] R. Idha, E. P. Sari, S. Humaidi, A. V H Simanjuntak, and U. Muksin, "Model Kecepatan Seismik 1-Dimensi Pada Wilayah Gempa Bumi Tarutung 2022 Mw 5.8," *Jurnal Penerapan Sistem Informatika (Komputer Manajemen)*, vol. 4, no. 2, pp. 469–477, 2023.
- [32] E. V. Cano, J. Akram, and D. B. Peter, "Automatic seismic phase picking based on unsupervised machine-learning classification and content information analysis," *Geophysics*, vol. 86, no. 4, pp. V299–V315, 2021, doi: 10.1190/geo2020-0308.1.